Kinetics of the Crystallization
of Barium Chromate[#]

M. S. Antonious, M. N. Ramsis, and A. O. Youssef

Chemistry Department, Faculty of Science, Ain Shams University, Abbassia, Cairo, Egypt

Summary. The kinetics of the crystallization of barium chromate have been studied conductometrically at 298 K for both spontaneous and seeded growth systems. The rate of growth follows a quadratic dependence upon the relative supersaturation which suggests a surface-controlled growth mechanism. This rate equation holds fairly well for the various supersaturation and solid/solution ratios used. The presence of seeds in the solution appears to accelerate the growth rate. Analysis of the calculated induction times in unseeded systems corroborates the surface-controlled growth mechanism. The effect of some additives on the kinetics of growth has also been studied. The retarding effect of these inhibitors is interpreted in terms of adsorption of inhibitor ions at the active crystal growth sites.

Keywords. Kinetics; Crystallization, Barium chromate; induction time.

Kinetik der Kristallisation von Bariumchromat

Zusammenfassung. Die Kinetik der Kristallisation von Bariumchromat wurde bei 298 K sowohl für Systeme mit spontanem als auch induziertem Kristallwachstum konduktometrisch untersucht. Die Wachstumsrate hängt quadratisch von der relativen Übersättigung ab, was einen oberflächenkontrollierten Wachstumsmechanismus nahelegt. Der erhaltene Ausdruck gilt verhältnismäßig gut für verschiedene Übersättigungsgrade und fest/flüssig – Verhältnisse. Die Gegenwart von Kondensationskeimen in der Lösung scheint die Wachstumsrate zu erhöhen. Eine Analyse der berechneten Induktionszeiten in nicht angeimpften Systemen bestätigt den oberflächenkontrollierten Wachstumsmechanismus. Der Effekt einiger Additive auf die Kinetik des Kristallwachstums wurde ebenfalls untersucht. Der verzögernde Effekt dieser Inhibitoren wird über die Adsorption von Ionen an den aktiven Wachstumsstellen erklärt.

Introduction

Numerous studies have been reported on the kinetics of crystal growth and dissolution of sparingly soluble alkaline-earth metal salts due to their participation in a wide number of biological, industrial, and environmental precipitation processes [1–3]. Of special interest are the barium salts [4–7] because of their importance in the petroleum industry as well as from the point of analytical chemical applications.

[#] Dedicated to the memory of Professor *E. N. Rizkalla* who passed away on November 29, 1993

Sparingly soluble salts can be precipitated *via* nucleation and growth from supersaturated aqueous solutions. The supersaturation is mostly achieved by rapid mixing of stable solutions containing the precipitating ions. Both diffusion- and surface-controlled growth mechanisms were suggested [8]. At high supersaturation ratios, the reaction was found to be determined by the rate of diffusion of the reacting species to the surface of the crystal, whereas at lower supersaturations the rate is controlled by a polynuclear surface-growth mechanism. The diversity in the order of the reaction from 1 to 4 in the case of barium sulfate crystallization [9–14] has led *Nancollas* and his group [15, 16] to study this system using a seeded-growth technique. Their results indicated second-order kinetics and a surface-controlled mechanism even at a supersaturation ratio as high as 56.

Induction-time determination is a well known method of characterizating the precipitation process of sparingly soluble salts [2, 6]. *Van der Leeden et al.* [17] gave a theoretical description of the induction time. *Sohnel* and *Mullin* [18] have analyzed the induction time resulting from various growth mechanisms.

This paper presents a systematic investigation of the precipitation kinetics of barium chromate, a system which to our knowledge has not been discussed before, over a wide range of supersaturation ratios from both spontaneous and seeded growth systems. The mechanism of precipitation in presence of additives is also discussed.

Results and Discussion

The rate of crystal growth, R, is given by equation 1

$$R = k(C - C_o)^n \qquad\qquad 1$$

where C and C_o are the actual and equilibrium concentrations and n is the order of the reaction. In our study, the rate of crystal growth in absence and presence of seeds and additives was analyzed using the following equation

$$R = -d[Ba^{++}]/dt = -d[CrO_4^{--}]/dt$$
$$= k_{obs}\{([Ba^{++}]_t[CrO_4^{--}]_t)^{1/2} - (\pi_s/f_2^2)^{1/2}\}^2 = k_{obs}\Delta^2 \qquad\qquad 2$$

where π_s is the thermodynamic solubility product (taken as $1.17 \times 10^{-10}\,mol^2 \cdot dm^{-6}$) [19], k_{obs} is the rate constant, and f_2 is the activity coefficient of the bivalent ion. Activity coefficients were calculated using the extended form of the *Debye-Hückel* equation proposed by *Davies* [20].

The supersaturation ratio, S, is defined as

$$S = (\pi/\pi_s)^{1/\delta} \qquad\qquad 3$$

where π is the ionic activity product and δ is the number of ions in the formula unit ($\delta = 2$ for $BaCrO_4$).

Plots of barium ion concentration, T_{Ba}, against time in the absence and presence of seeds are shown in Figs. 1 and 2, and the results obtained by crystal-growth experiments are summarized in Tables 1 and 2. The values of k_{obs} were obtained by plotting the integrated form of equation 2:
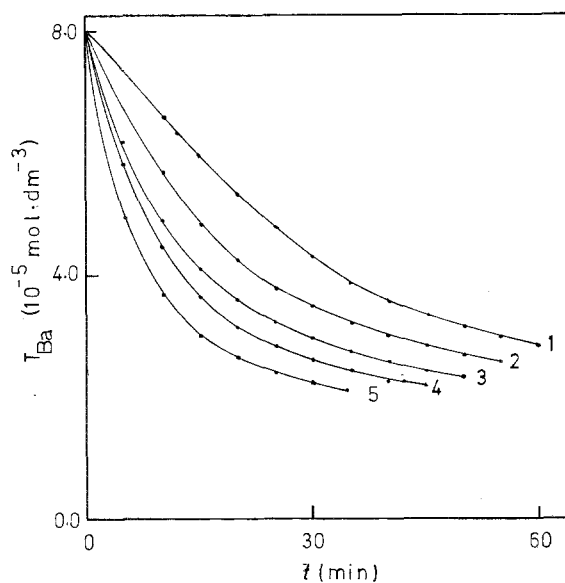
$$k_{obs} \cdot t = \Delta_t^{-1} - \Delta_i^{-1} \qquad\qquad 4$$

Fig. 1. Growth curves for $BaCrO_4$ in absence and presence of different amounts of seed A; $T_{Ba} = T_{CrO_4} = 8 \times 10^{-5}\,M$; curve 1: unseeded; 2: $1.6 \times 10^{-5}\,M$; 3: $4.8 \times 10^{-5}\,M$; 4: $8.0 \times 10^{-5}\,M$; 5: $11.2 \times 10^{-5}\,M$
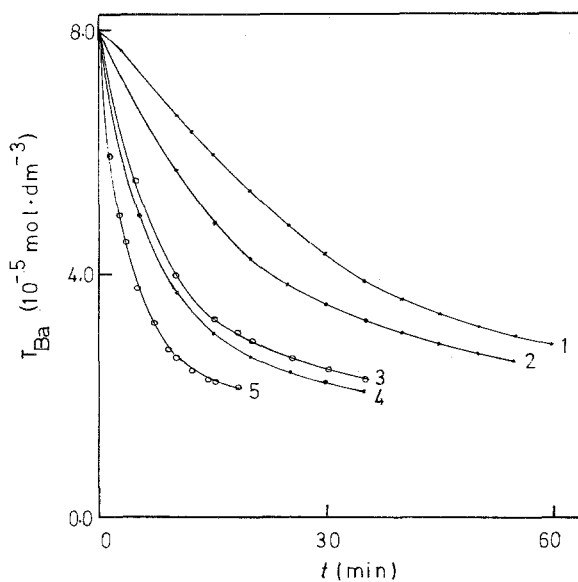

Fig. 2. Growth curves for $BaCrO_4$ in absence and presence of seeds A and B; $T_{Ba} = T_{CrO_4} = 8 \times 10^{-5}\,M$; curve 1: unseeded; 2: $1.6 \times 10^{-5}\,M$ seed A; 3: $1.6 \times 10^{-5}\,M$ seed B; 4: $11.2 \times 10^{-5}\,M$ seed A; 5: $11.2 \times 10^{-5}\,M$ seed B

Here, Δ_t and Δ_i represent the concentration functions at time t and time 0, respectively. These plots are characterized by an initial slow surge of growth (induction time, t) the duration of which is a function of the supersaturation ratio (see Fig. 3). The induction time is defined as the time elapsing between the creation of the supersaturation and the formation of a visually detectable quantity of the precipitate. At the end of this surge, the linear conditions of equation 4 are fulfilled up to a degree of reaction (θ) of at least 85%. The induction time decreases sharply by increasing supersaturation ratio and/or by adding seeds.

Table 1. Crystallization of barium chromate from super-saturated solution at 298 K in the absence of seeds; $T_{Ba}^a = T_{CrO_4}$

T_{Ba} $(10^{-5} M)$	S	k_{obs} $(10^3 M^{-1}\cdot min^{-1})$	t^b (min)
8.0	7.39	0.840	10.06
10.0	9.24	1.096	3.75
12.0	11.09	1.421	3.32
15.0	13.86	2.149	1.70
20.0	18.49	3.563	1.19
25.0	23.11	6.361	0.70

[a] T_{Ba} and T_{CrO_4} represent the initial barium and chromate ion concentrations, respectively; [b] Induction time

Table 2. Crystallization of barium chromate from supersaturated solution at 298 K in presence of seeds A and B; $T_{Ba} = T_{CrO_4}$

T_{Ba} $(10^{-5} M)$	S	Seed type	Seed concn. $(M\cdot 10^{-5})$	k_{obs} $(10^3 M^{-1}\cdot min^{-1})$
8.0	7.39	A	1.6	0.999
8.0	7.39	A	4.8	1.372
8.0	7.39	A	8.0	1.794
8.0	7.39	A	11.2	2.540
8.0	7.39	B	1.6	2.059
8.0	7.39	B	4.8	2.695
8.0	7.39	B	8.0	3.813
8.0	7.39	B	11.2	5.211
10.0	9.24	A	1.6	1.330
10.0	9.24	B	1.6	3.198
12.0	11.09	A	1.6	1.643
12.0	11.09	B	1.6	4.003

A further experiment was also necessary to observe the effect of mixing non-stoichiometric amounts of barium chloride and potassium chromate solutions. This resulted in a small acceleration of the rate of crystallization and an appreciable decrease in the induction time. Thus, when $T_{Ba} = 3/2\cdot T_{CrO_4} = 15 \times 10^{-5} M$, the rate constant was $1.558 \times 10^3 M^{-1}\cdot min^{-1}$, whereas if $T_{Ba} = 2/3\cdot T_{CrO_4} = 10 \times 10^{-5} M$, the rate constant was $1.495 \times 10^3 M^{-1}\cdot min^{-1}$. Although in both cases the super-saturation ratio was the same ($S = 11.32$), yet the rate constant differed. The induction time was also found to vary and to be equal to 0.47 min for the former and 1.08 min for the latter case. These two values parallel the values obtained for their rate constants. In general, for a second-order reaction the rate determining step could be expressed as
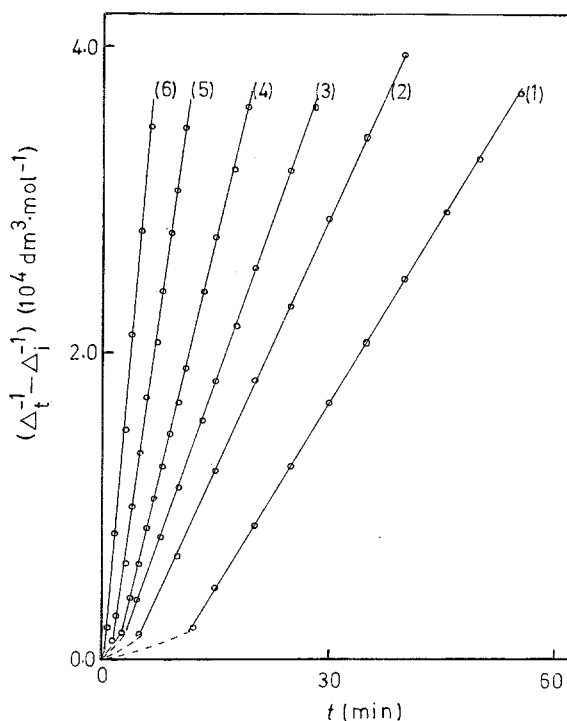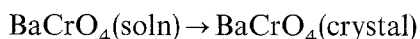
$$Ba^{++}(soln) + CrO_4^{--}(soln) \rightarrow BrCrO_4(crystal)$$
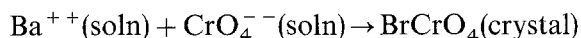
Fig. 3. Plots of the integrated form of equation 2 for the growth of $BaCrO_4$ at different concentrations for Ba^{++}; $T_{Ba} = T_{CrO_4}$; curve 1: $8 \times 10^{-5} M$; 2: $10 \times 10^{-5} M$; 3: $12 \times 10^{-5} M$; 4: $15 \times 10^{-5} M$; 5: $20 \times 10^{-5} M$; 6: $25 \times 10^{-5} M$

or

$$BaCrO_4(soln) \rightarrow BaCrO_4(crystal)$$

In presence of an excess common ion, the latter tends to adsorb more readily on active sites or crystal imperfections than the neutral ion pairs. This process would perhaps lead to a highly charged surface which in turn enhances the adsorption of barium chromate ion pairs, thus increasing the rate constant.

These results are consistent with a second-order crystallization kinetics, as shown in Figs. 3 and 4. The agreement of the growth rate data with a parabolic rate law (equation 4) over the big range of supersaturation ratios and seed/solution ratios used rules out bulk diffusion of the electrolyte to the crystal surface as the rate determining step and is indicative of a surface-controlled growth mechanism.

An alternative approach is to interpret the kinetics of precipitation in terms of Nielsen's chronomal analysis [21]. For diffusion-controlled precipitation, θ vaires with time following the relationship

$$K_D t = \int_0^\theta \theta^{-1/3}(1 - \theta)^{-1}d\theta = I_D, \qquad 5$$

whereas for polynuclear surface-controlled growth

$$K_P t = \int_0^\theta \theta^{-2/3}(1 - \theta)^{-P}d\theta = I_P \qquad 6$$

where P is the order of the reaction and K_P and K_D are constants related to the final particle size and the initial concentration. The appropriate mechanism as well as the
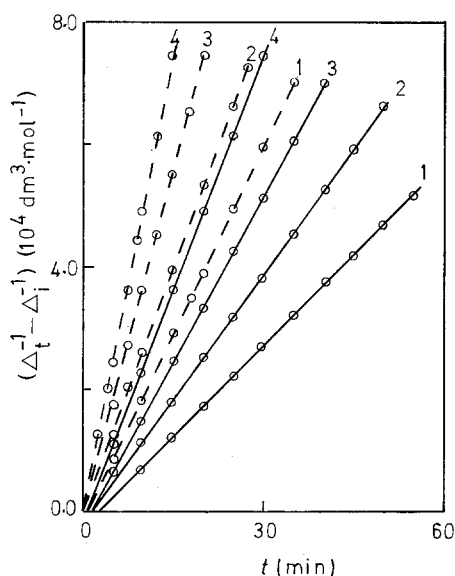
Fig. 4. Plots of the integrated form of equation 2 for the growth of $BaCrO_4$ at different amounts of seeds **A** (——) and seeds **B** (- -); $T_{Ba} = T_{CrO_4} = 8 \times 10^{-5} M$; curve 1: $1.6 \times 10^{-5} M$; 2: $4.8 \times 10^{-5} M$; 3: $8.0 \times 10^{-5} M$; 4: $11.2 \times 10^{-5} M$

order of the reaction can be inferred from plots of I (obtained from θ) against time. These plots are shown in Fig. 5 for growth from unseeded and seeded solutions. For an unseeded system, only the I_2 mechanism fulfills the linearity condition of equation 6 with an order of reaction of 2. The linearity condition appears to be limited to the late stages of growth (θ ranging from 25%–85%). The nonlinearity in the low θ ranges may suggest a different operating mechanism of growth. A similar behaviour has been observed for the crystallization of calcium oxalate [3]. In presence of seeds, none of the curves completely fulfills the conditions of equations 5 or 6. However, combination of the surface- and diffusion-controlled mechanisms in this case could fulfill the linear conditions over the entire range of θ, regardless of the value of P. The deviation from linearity may be also due to the hypothesis behind the chronomal analysis which presumes homogeneous nucleation and formation of uniformly spherical particles [21].

The growth of barium chromate in the presence of seeds leads to (a) an increase in the observed rate constant, as indicated from Tables 1 and 2, with an extent of increase proportional to the amount of seed present, and (b) to the diminishing of the induction time as observed from Figs. 3 and 4. According to the nucleation theories, in pure solutions a fraction of the lattice ions is consumed in forming the embryos which function as a base for the actual growth stage, whereas in seeded systems the added seed presents suitable sites for direct growth. This accounts for the slow surge observed in the integrated rate plots in the case of spontaneous growth which diminishes upon adding seeds.

The difference in the values of the observed rate constants in the presence of seeds **A** and **B** indicates that seed **B** has more crystalline perfections leading to an acceleration of the rate of crystal growth as shown in Table 2. Obviously, the reason is due to the difference in the way of preparation of both seeds where seed **B** was allowed to age with the mother liquour for three weeks in the course of its preparation leading to more clean facets seeds and more active sites for growth. In
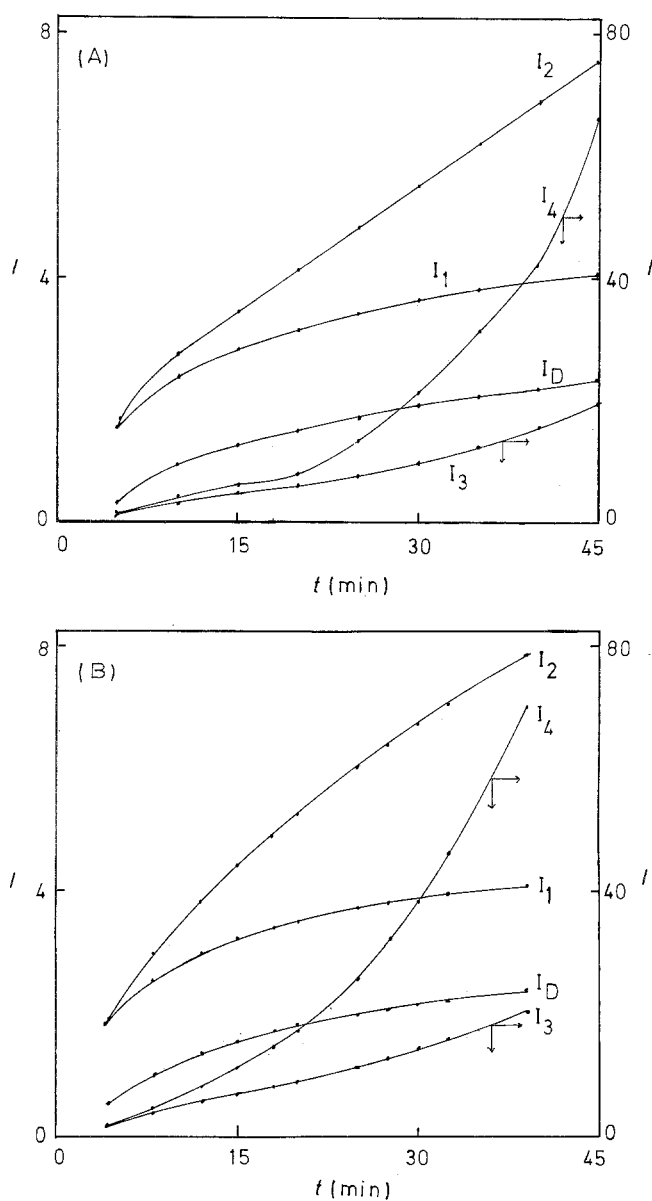
Fig. 5. Plots of I_D and I_P ($P = 1$–4) chronomals as a function of time for $BaCrO_4$ precipitation; A: $T_{Ba} = T_{CrO_4} = 10 \times 10^{-5} M$; **B:** $T_{Ba} = T_{CrO_4} = 10 \times 10^{-5} M$; [seed **A**] = 0.4×10^{-5} mol

case of seed **A**, its direct separation from its mother liquour immediately after preparation has led to a relatively imperfect structure, thus leading to a lower number of active sites for growth. Thus, we can conclude that the presence of seed **B** during crystal growth will markedly affect the growth rate, while the presence of seed **A** can be considered as a progressive primary nucleation stage of crystallization with unseeded conditions. This conclusion is supported by observing the relation between the logarithm of the rate constant and the seed concentration (Fig. 6), where the value of $\log k$ for unseeded system lies on the extrapolation of the straight line resulting with seed **A**.

A commonly used parameter to characterize the crystallization process is the induction time. Several techniques were applied for induction time determination
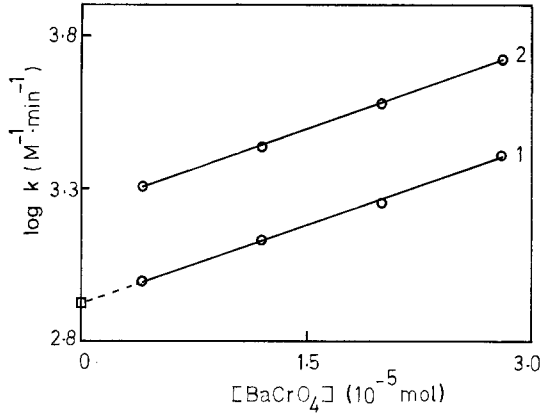
Fig. 6. Plot of $\log K$ for $BaCrO_4$ vs. different amounts of seed **A** (curve 1) and seed **B** (curve 2); $T_{Ba} = T_{CrO_4} = 8 \times 10^{-5} M$; the value of $\log k$ for the unseeded system is given as □

[18, 22–25]. The simplest one is that obtained from the intercept of the integrated form of equation 2 with the time axis. Recently, a general expression for the induction time in unseeded crystal growth has been proposed and claimed to be valid for any number of nuclei growing in a supersaturated solution [6]. This expression for t_u (induction time of unseeded system) leads to

$$F_u(S) = LnA_u + B/nLn^2S \qquad\qquad 7$$

where

$$F_u(S) = Ln[S^{1/n}(S-1)^{(n-1)/n}t_u] \qquad\qquad 8$$

for normal or volume diffusion-controlled growth, or

$$F_u(S) = Ln[S^{1/n}(S-1)^{2(n-1)/n}t_u] \qquad\qquad 9$$

for spiral growth. A_u is a single factor, independent from S. In these three cases of growth, plots of F_u vs. $1/Ln^2S$ should give a straight line. The quality of the fit for each possible value of n gives information about the operating growth mechanism and the most likely value of n.

For two-dimensional nucleation mediated growth, F_u is presented as

$$F_u(S) = LnA_u + (n-1)B/3nLnS + B/nLn^2S, \qquad\qquad 10$$

in which

$$F_u(S) = Ln[(S-1)^{2(n-1)/3n}S^{(n+2)/3n}t_u] \qquad\qquad 11$$

Accordingly, the relation between F_u and $1/LnS$ can be fitted by a parabolic dependence, and the quality of the fit is indicated by the value of n.

Our results failed to obtain a reasonable straight line for $F_u(S)$ vs. $1/Ln^2S$, thus eliminating normal, spiral, and volume diffusion-controlled mechanisms. However, they gave an excellent correlation (c.c. 0.998) for the two-dimensional nucleation-mediated growth ($n = 2$) with the parabolic equation
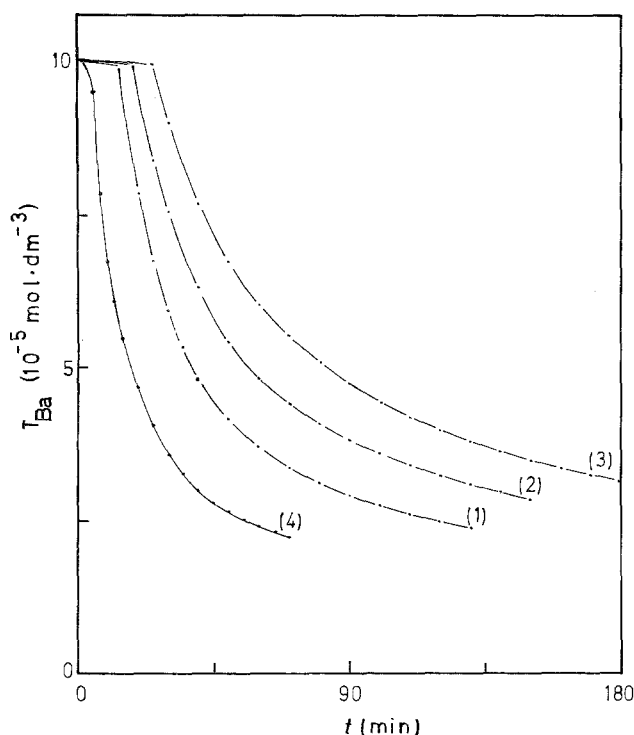
$$F(S) = 10.84 - 43.17/LnS + 59.88/Ln^2S$$

Fig. 7. Growth curves for barium chromate in the presence of $1 \times 10^{-7} M$ solution of additives; curve 1: $ENTMP$; 2: STP; 3: $HEDP$; 4 (for comparison): no additives; $T_{Ba} = T_{CrO_4} = 1 \times 10^{-4} M$

In the above analysis, the induction time in the case of the highly supersaturated solution ($S = 23.11$) was eliminated, since at very high saturation ratios the induction time is too small to be indicated precisely with the above mentioned technique.

The effect of additives on the kinetics of precipitation of the barium chromate was also studied. Plots of barium ion concentration against time for typical growth experiments in the presence of additives are shown in Figs. 7 and 8. The small changes in concentration of barium ions due to its complexation with the additives were neglected in the rate calculations since their contribution to the total barium content was at the most less than 0.1%. Values of the observed rate constants in presence of additives are given in Table 3.

As in the case of both spontaneous and seeded growth systems, the results obtained in presence of additives are also consistent with second order crystallization kinetics as indicated in Figs. 9 and 10. The figures indicate that induction times are now more prolonged than in case of spontaneous growth.

As the concentration of additive increases, the active sites for crystallization on the crystal surface are blocked through adsorption, and consequently the growth rate decreases. Differences in the inhibiting action of additives can be attributed to structural factors such as their size. Adsorption-rate measurements of STP on strontium sulfate precipitated from pure solution showed that adsorption of STP takes place soon after the birth of 17 Å nuclei in a solution containing polyphosphate [26]. Extending this conclusion to other phosphonate systems, it would be expected that adsorption of the larger molecule $ENTMP$ is likely to take place after the birth of larger aggregates of the host lattice, whereas with the $HEDP$ molecule nuclei of
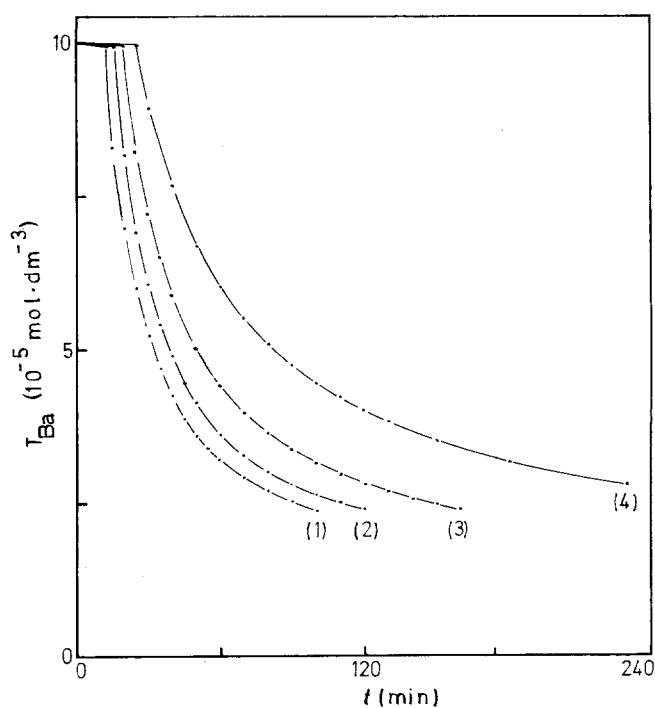
Fig. 8. Growth curves for barium chromate in presence of different concentrations of *HEDP* as additive; curve 1: $1.0 \times 10^{-8} M$; 2: $2.0 \times 10^{-8} M$; 3: $4.0 \times 10^{-8} M$; 4: $10 \times 10^{-8} M$; $T_{Ba} = T_{CrO_4} = 1.0 \times 10^{-4} M$

Table 3. Effect of additives on the rate of growth of barium chromate at 298 K; $T_{Ba} = T_{CrO_4}$

| T_{Ba} $(10^{-5} M)$	S	Additive	Additive conc. $(10^{-8} M)$	k_{obs} $(10^3 M^{-1} \cdot min^{-1})$
10.0	9.24	*ENTMP*	1.0	0.998
10.0	9.24	*ENTMP*	2.0	0.918
10.0	9.24	*ENTMP*	4.0	0.811
10.0	9.24	*ENTMP*	10.0	0.583
12.0	11.09	*ENTMP*	10.0	0.715
15.0	13.86	*ENTMP*	10.0	0.877
10.0	9.24	*STP*	1.0	0.885
10.0	9.24	*STP*	2.0	0.721
10.0	9.24	*STP*	4.0	0.550
10.0	9.24	*STP*	10.0	0.344
12.0	11.09	*STP*	10.0	0.394
15.0	13.86	*STP*	10.0	0.466
10.0	9.24	*HEDP*	1.0	0.764
10.0	9.24	*HEDP*	2.0	0.616
10.0	9.24	*HEDP*	4.0	0.414
10.0	9.24	*HEDP*	10.0	0.238
12.0	11.09	*HEDP*	10.0	0.267
15.0	13.86	*HEDP*	10.0	0.313
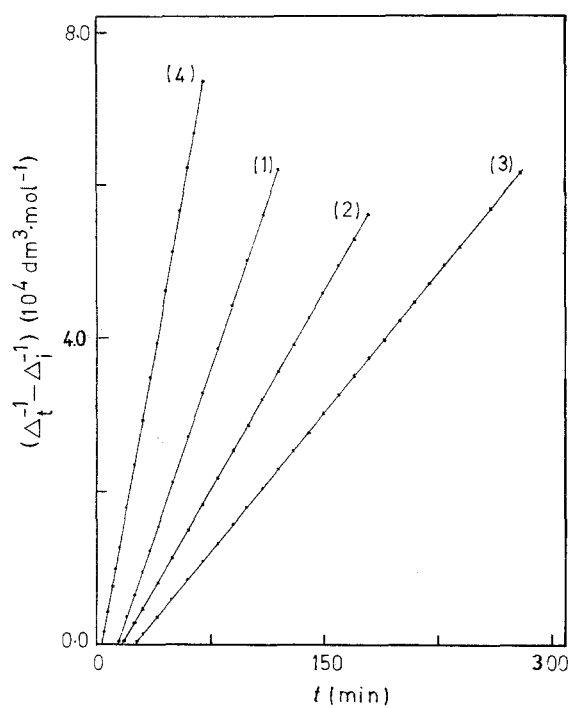
Fig. 9. Plots of the integrated form of equation 2 in presence of $1 \times 10^{-7} M$ of additives; $T_{Ba} = T_{CrO_4} = 1.0 \times 10^{-4} M$; curve 1: *ENTMP*; 2: *STP*; 3: *HEDP*; 4 (for comparison): no additives
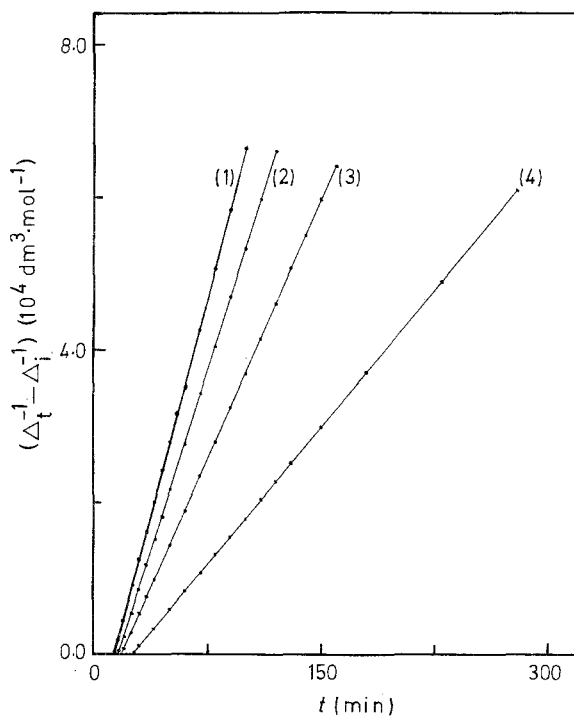

Fig. 10. Plots of the integrated form of equation 2 for different concentrations of *HEDP* as additive; $T_{Ba} = T_{CrO_4} = 1.0 \times 10^{-4} M$; curve 1: $1.0 \times 10^{-8} M$; 2: $2.0 \times 10^{-8} M$; 3: $4.0 \times 10^{-8} M$; 4: $10 \times 10^{-8} M$

smaller dimensions would fulfill the adsorption requirements. This order holds well with the results obtained for the three additives studied in this work.

Experimental

All chemicals used were analytical grade reagents and were always freshly prepared before use. Stock solutions were prepared in low conductivity water (doubly distilled, deionized water) and diluted as required. The exact molarities of barium and chromate ions were checked using standard analytical methods [27].

The additives used were: sodium tripolyphosphate (*STP*), ethylenediaminetetramethylenephosphonic acid (*ENTMP*), and 1-hydroxyethylidene-1,1-diphosphonic acid (*HEDP*). Both *ENTMP* and *HEDP* were kindly provided by Monsanto Industrial Chemicals, Brussels, Belgium. Commercial grade *STP* was purified four times from a methanol-water mixture [28]. The purity of the final porduct ($Na_5P_3O_{10} \cdot 6H_2O$) was checked by elemental analysis.

Barium chromate seeds were prepared by two different methods: seed **A** was obtained as the spontaneously precipitated solid formed by direct addition of 0.01 *M* barium chloride solution to a 0.01 *M* potassium chromate solution. The solid was filtered at once, washed, and dried overnight at 383 K. Seed **B** was prepared precisely in the same way as seed **A** with the exception that the precipitated solid was allowed to age with the mother-liquor at 298 K for three weeks; it was then filtered, washed, and dried at 383 K.

Scanning electron microscopic (SEM) indicated that barium chromate seeds are in the form of microcrystallites and that seed **B** is more ordered than seed **A**. X-ray diffraction studies showed that seeds of type **B** exhibit a higher degree of crystallinity relative to those of type **A**. Surface area measurements gave a surface area of 0.9 and 1.7 m^2/g for seeds **A** and **B**, respectively.

The conductance measurements were carried out using an YSI model 32 conductance meter with a limiting accuracy of 1×10^{-7} mho. The measurements were carried out under controlled temperature (298 ± 0.1 K) using a water circulating constant-temperature bath. The volume of the reaction mixture was always kept constant at 250 cm^3. The cell constant was measured to be 0.15437 cm^{-1}. Potassium chromate was always added to barium chloride solution. Seeds or additives, if present, were added to the barium chloride solution. The changes of concentration in the solution were calculated assuming a constant equivalent conductivity of barium chloride of 139.9 $ohm^{-1} \cdot equiv^{-1} \cdot cm^2$ at 298 K [19].

Correction of conductivity due to the potassium chloride formed was taken into consideration. For experiments conducted in the presence of additives, a blank experiment was necessary to correct for their contribution to the total conductance.

References

[1] Costa-Bauza A, Grases F, Sohnel O (1993) Cryst Res Technol **28**: 337
[2] Verdoes D, Kashchiev D, Van Rosmalen GM (1992) J Crystal Growth **118**: 401
[3] Rizkalla EN, Moawad MM (1984) J Chem Soc Faraday Trans 1, **80**: 1617
[4] Symeopoulos BD, Koutsoukos PG (1993) Appl Radiat Isot **44**: 894
[5] van der Leeden MC, Kashchiev D, van Rosmalen GM (1993) J Crystal Growth **130**: 221
[6] van der Leeden MC, Kashchiev D, van Rosmalen GM (1992) J Colloid Interface Sci **152**: 338
[7] Nielsen AE (1961) Acta Chem Scand **15**: 441
[8] Nielsen AE (1958) Acta Chem Scand **12**: 951
[9] Gunn DF, Murthy MS (1972) Chem Eng Sci **27**: 1293
[10] Condin L (1972) Talanta **19**: 945
[11] Pleckach LI (1971) Zh Anal Khim **26**: 2290
[12] Condin L (1970) Talanta **17**: 1053
[13] Walton AG, Hlabse T (1963) Anal Chim Acta **29**: 249

[14] Nielsen AE (1955) J Colloid Sci **10**: 576

[15] Nancollas GH, Liu ST (1975) Soc Pet Eng J **15**: 509

[16] Liu ST, Nancollas GH (1975) J Colloid Interface Sci **52**: 582

[17] van der Leeden MC, Verdoes D, Kashchiev D, van Rosmalen GM (1991) Garside J, Davey RJ, Jones AG (eds) Advances in industrial crystallization. Butterworth-Heinemann, London, p 31

[18] Söhnel O, Mullin JW (1988) J Colloid Interface Sci **123**: 43

[19] Handbook of chemistry and physics, 74th edn (1993)

[20] Davies CW (1962) Ion association. Butterworths, London

[21] Nielsen AE (1964) Kinetics of precipitation. Pergamon Press, Oxford

[22] Kubota N, Takadi T, Kawakami T (1986) J Crystal Growth **74**: 259

[23] Wojcieckowski K, Kibalczyc W (1986) J Crystal Growth **76**: 379

[24] Söhnel O, Mullin JW (1979) Krist Technik **14**: 217

[25] Söhnel O, Mullin JW (1978) J Crystal Growth **44**: 377

[26] Naono H (1967) Bull Chem Soc Japan **40**: 1104

[27] Bassett J, Denney RC, Jeffery GH, Mendham J (1978) Vogel's textbook of quantitative inorganic analysis, 4th edn. Longmans, London

[28] Quimby QT (1954) J Phys Chem **58**: 603